

## Dissociative scattering of $\text{H}_3^+$ molecular ions from the Si(100) surface

Hiroyuki Hirayama

*Microelectronics Research Laboratories, NEC Corporation, 34 Miyukigaoka, Tsukuba 305, Japan*

(Received 2 April 1993; revised manuscript received 17 May 1993)

Dissociative scattering of  $\text{H}_3^+$  molecular ions from the Si(100) surface has been studied with incident energies from 450 to 1500 eV. At all these energies,  $\text{H}_3^+$  was found to dissociate upon collision with the Si(100) surface. In the energy spectrum of the scattered  $\text{H}^+$  ion fragment, a large background is observed on the low-energy side of the surface peak for the incident energies above 1000 eV, whereas the background disappears for the incident energies below 1000 eV. With the reduction of the background, the angular distribution of intensity of the surface-scattered  $\text{H}^+$  fragments becomes more specular. In addition, at high energies the peak energy of the  $\text{H}^+$  fragment corresponds well with that expected for binary scattering between a  $\text{H}_3^+$  molecular ion and a single Si atom. However, at low energies the peak energy is higher than would be expected by this model. All these changes indicate that the scattering mode changes from binary collisions at high incident energy to surface scattering at low incident energy, where the incident  $\text{H}_3^+$  interacts via the long-range potential of many surface Si atoms. Even at the lowest incident energy, the scattered  $\text{H}^+$  energy spectrum has a finite-energy width, although it decreased with the incident energy. This energy width is caused by the release of the kinetic energy upon dissociative scattering. The observed distribution of the released energy indicates the impulsive feature of the dissociation.

### I. INTRODUCTION

In dry processes for ultralarge scale integrated (ULSI) semiconductor device fabrication, control of chemical reactions between atoms, molecules, ions, and surfaces is important. The low-energy (below a few hundred eV) ion-beam technique is especially promising, since it can overcome the potential barrier for a chemical reaction, which is difficult or impossible for a thermal reaction, with negligible damage to the surface.<sup>1</sup> Among ion/surface systems,  $\text{H}^+$ /Si is one of the most important, because of the strong interaction of hydrogen with Si surface dangling bonds.<sup>2-4</sup> However, due to the large neutralization probability of  $\text{H}^+$ , neutralization occurs both on the incoming and outgoing trajectories in  $\text{H}^+$ /Si scattering experiments. This complicates understanding the reaction through observing the scattered  $\text{H}^+$  yield. To avoid this complication, we have started a study of the  $\text{H}_3^+$ /Si(100) system.<sup>5</sup> In our previous work, 1200 eV  $\text{H}_3^+$  was found to be dissociatively scattered from the Si(100) surface. The scattering angle dependence of the scattered  $\text{H}^+$  surface peak energy agrees with a model in which the  $\text{H}_3^+$  dissociates *after* binary collision with a surface Si atom. Therefore,  $\text{H}^+$  is generated only on the outgoing path, making the interpretation of the  $\text{H}^+$  yield much easier in the  $\text{H}_3^+$ /Si(100) system.

For the application of ion beams to device processing, the energy regime below 1000 eV is most important. However, in spite of its importance, the interaction in this energy range is not fully understood; especially, few studies have been reported for the molecular ion-surface interaction.<sup>1</sup> Generally, scattering phenomena in such a low-energy regime are very complicated. By reducing the incident energy, the scattering mode is expected to

change from binary collision between the incident ions and individual surface atoms at the high-energy extreme<sup>6</sup> to simultaneous many-body interactions between each ion and the surface atoms at the low-energy extreme.<sup>7</sup> Moreover, for molecular ions, a critical incident energy for dissociative scattering has been reported in  $\text{N}_2^+$ /Pt(100) (Ref. 8) and  $\text{CO}^+$ /Pt(100),<sup>9</sup> but the dissociation mechanism is not yet clear. The dissociation is attributed to classical translational-vibrational energy transfer in  $\text{N}_2^+$ ,  $\text{CO}^+$ /Pt(100),<sup>8,9</sup> whereas it is attributed to the electronic transition in  $\text{N}_2^+$ /gold,<sup>10</sup>  $\text{N}_2^+$ /Ni(111),<sup>11</sup> and  $\text{H}_2^+$ /Al(100),<sup>12</sup> Ni(111).<sup>13</sup> A strong dependence of the neutralization on the ionic character of the surface atom has been reported in the low-energy regime.<sup>14,15</sup> In this paper, we report the energy dependence of the  $\text{H}_3^+$  scattering mode from the Si(100) surface. The scattering mode change is discussed using results of the angular-resolved  $\text{H}^+$  energy spectrum at various energies. At high energies, the  $\text{H}_3^+$  is scattered in binary collision mode, whereas it "feels" many-body interactions with surface atoms at low energies. The dissociation mechanism is also discussed from the observed energy spectrum shape. The broad kinetic-energy distribution of the scattered  $\text{H}^+$  fragment comes from the internal energy release into kinetic energy upon the dissociative scattering. The kinetic-energy release is caused by the internal energy excitation of the  $\text{H}_3^+$  molecular ion at the closest encounter of the scattering.

### II. EXPERIMENT

The experimental setup consists of an ion-beam line and an ultrahigh-vacuum (UHV) scattering chamber. The details of the experimental setup have been described

previously.<sup>5</sup> Here we briefly explain the setup.  $\text{H}_3^+$  ions are extracted from a  $\text{H}_2$  plasma ion source. From the several ion species present,  $\text{H}_3^+$  ions are selected by an  $E \times B$  filter, and neutrals are eliminated from the ion beam by a  $7^\circ$  deflecting electrode. The beam energy is controlled by a Menzinger-type decelerator. The scattered ion energy spectrum is detected by an electrostatic spherical deflector analyzer with an energy resolution of 1 eV. The analyzer is rotatable around the Si(100) sample mounted on a 6-axis goniometer. The sample was thermally cleaned in the UHV chamber, and the cleanliness was confirmed by observing a sharp  $2 \times 1$  reflection high-energy electron-diffraction (RHEED) pattern of the Si(100) surface. The RHEED pattern was also used to align the scattering azimuth along the [110] direction.

### III. RESULTS AND DISCUSSION

#### A. Scattering mode change with the incident energy

Figure 1 shows the dependence of the scattered ion energy spectrum on the incident  $\text{H}_3^+$  energy for the Si(100) surface. All the spectra were measured at  $60^\circ$  incident and  $60^\circ$  exit angles from the surface *parallel* direction. The scattering was observed along the [110] azimuthal direction. The most remarkable character of the spectra is that the peak ion intensity is always found at an energy less than  $\sim \frac{1}{3}$  of the incident energy. This indicates that  $\text{H}_3^+$  is dissociatively scattered.<sup>16</sup> Specifically, the incident  $\text{H}_3^+$  is scattered with a Si atom and then dissociates, and the resulting  $\text{H}^+$  ion fragment, which has the kinetic energy of  $\frac{1}{3}$  of the scattered  $\text{H}_3^+$ , was detected by the analyzer.

At incident energies above 1000 eV, the scattered  $\text{H}^+$  spectrum shows a broad structure on the low-energy side, which disappears for incident energies below 1000 eV. For incident energies below 1000 eV, the scattered  $\text{H}^+$  spectrum shows a single, Gaussian-like peak. In our previous study of 1200 eV  $\text{H}_3^+$  scattering from the Si(100) surface, the scattered  $\text{H}^+$  spectrum was found to consist of a surface peak at  $\frac{1}{3}$  the energy of the binary scattered  $\text{H}_3^+$  with the Si atom, and a broad structure at lower energy.<sup>5</sup> The broad structure at lower energy is due to the  $\text{H}^+$  ions scattered from bulk after repeated inelastic scattering inside the crystal.<sup>6</sup> Figure 2 shows the exit angle dependence of the  $\text{H}^+$  fragment energy spectrum. In this case, the incident energy of  $\text{H}_3^+$  was 1200 eV and the incident angle was  $60^\circ$ . As shown in the figure, the surface-scattered structure is clear for exit angles close to the surface *parallel*. In Figure 2, arrows indicate the energy expected for the  $\text{H}^+$  fragment, which is generated by the dissociation of a binary scattered  $\text{H}_3^+$  with a Si atom. As reported in our previous study,<sup>5</sup> observed surface peaks agree with the arrows in the 1200-eV incident  $\text{H}_3^+$  scattering. At large exit angles, the bulk-scattered feature dominates the surface-scattered peak. This effect is significant at the exit angle of  $60^\circ$ , where the spectrum of Fig. 1 was measured. Therefore, all the broad structures for incident energies above 1000 eV in Fig. 1 are considered to be the superposition of the small surface-

scattered peak and the dominant bulk-scattered feature. However, the spectral change in Fig. 1 indicates that the relative intensity of the surface-scattered  $\text{H}^+$  to the bulk-scattered  $\text{H}^+$  becomes larger with reducing the incident energy of  $\text{H}_3^+$ . Finally, at incident energies below 1000 eV, only the surface-scattered peak is observed. This continuous change in the spectra suggests that the penetration power of the incident  $\text{H}_3^+$  decreases rapidly with decreasing incident energy.

In Fig. 1, the energy of the surface-scattered peak energy shifts obviously from  $\frac{1}{3}$  the energy of the binary scattered  $\text{H}_3^+$  toward the higher-energy side at low incident energies. The dependence of the shift on the incident energy is shown in Fig. 3, normalized to  $\frac{1}{3}$  the energy of  $\text{H}_3^+$ . In the figure,  $\frac{1}{3}$  of the normalized energy expected for the binary scattering of  $\text{H}_3^+$  with a Si atom, a  $\text{Si}_2$  cluster, and a  $\text{Si}_3$  cluster are also indicated by broken lines. For 1200-eV scattering, the peak agrees with the energy expected for dissociation after the binary collision

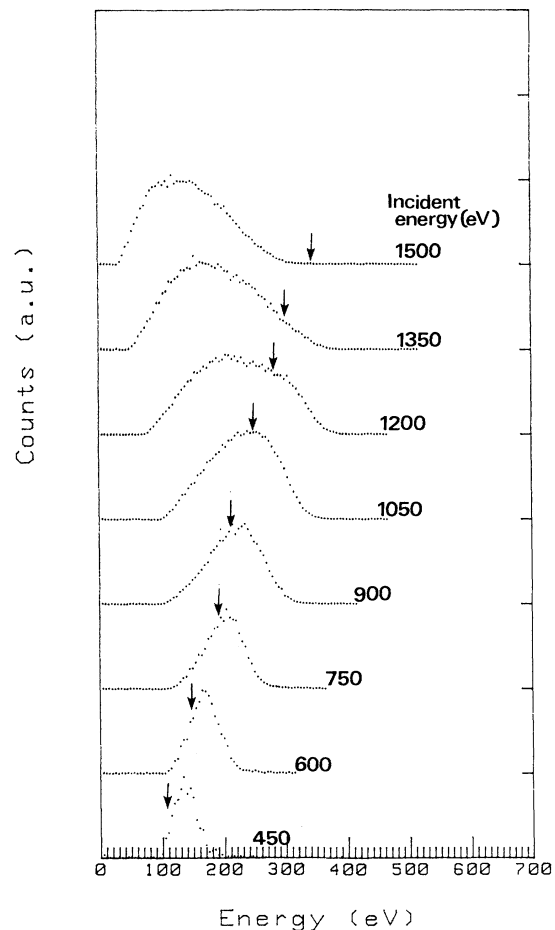


FIG. 1. Incident energy dependence of the scattered  $\text{H}^+$  energy spectrum. Both the incident and the exit angles were  $60^\circ$  measured from the surface *parallel*. The incident energy was indicated in the figure. Arrows indicate the energies of the  $\text{H}^+$  fragment expected from the model in which the incident  $\text{H}_3^+$  is binary scattered from a surface Si atom and then dissociates into  $\text{H}^+$ .

of  $H_3^+$  with a surface Si atom. However, the normalized energy increases continuously with decreasing incident energy. This change is interpreted as due to an increase in the corresponding number of Si atoms interacting with the incident  $H_3^+$ . Hence, the scattering cross section of the surface scattering is large for the  $H_3^+$  of the low incident energy. This explains the observed disappearance of the bulk-scattered feature at low  $H_3^+$  incident energy.

Figures 4 and 5 show the exit angle dependence of the scattered  $H^+$  fragment energy spectra with 900- and 600-eV incident  $H_3^+$ , respectively. For these low incident energies, the surface-scattered peak is observed only at exit angles around  $60^\circ$ , the same as the incident angle; the scattering is thus specular. In contrast, for 1200-eV incident ions, the surface-scattered peak intensity is large at exit angles close to the surface parallel (Fig. 2). However, at such a high incident energy, the bulk scattering is superimposed on the surface-scattered peak. To better analyze the exit angle dependence of the surface-scattered  $H^+$  intensity, we deconvoluted the  $H^+$

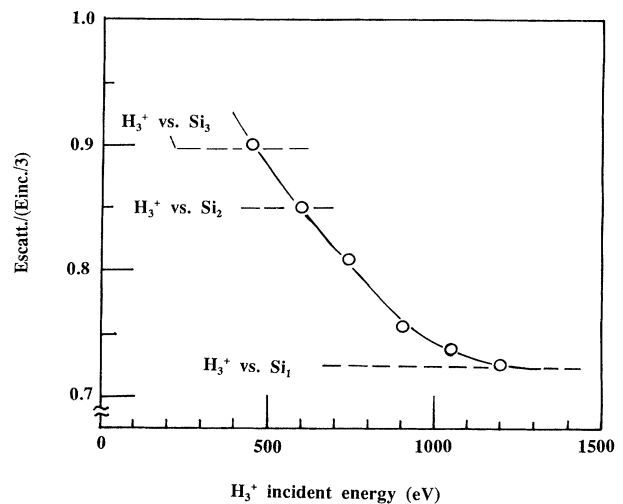


FIG. 3. Incident energy dependence of the surface-scattered  $H^+$  energy. The energy of the peak intensity of the surface-scattered  $H^+$  fragment is normalized to  $\frac{1}{3}$  the energy of the incident  $H_3^+$ .

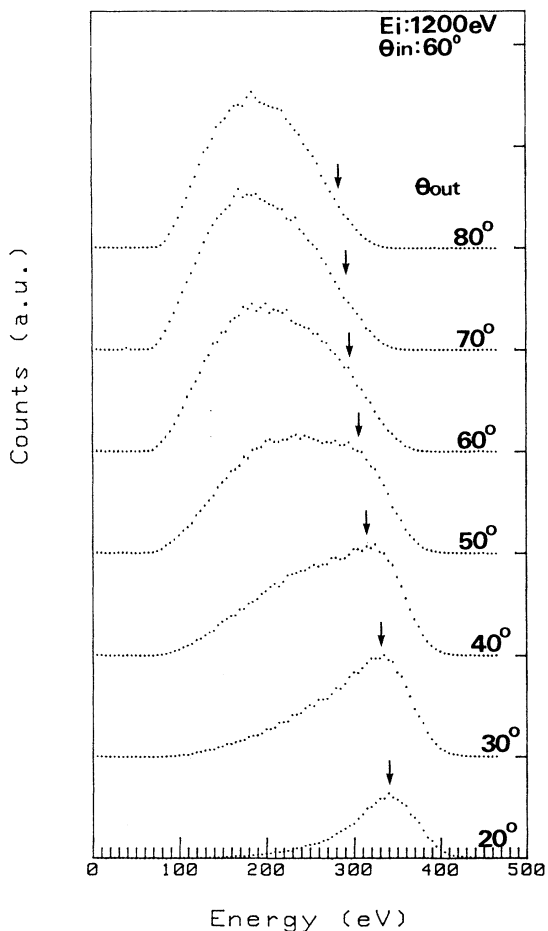


FIG. 2. Exit angle dependence of the scattered  $H^+$  fragment energy spectrum. The incident angle of 1200 eV  $H_3^+$  was  $60^\circ$ . Arrows indicate the energy of the  $H^+$  fragment expected in the model in which the incident  $H_3^+$  is binary scattered with a surface Si atom and then dissociates.

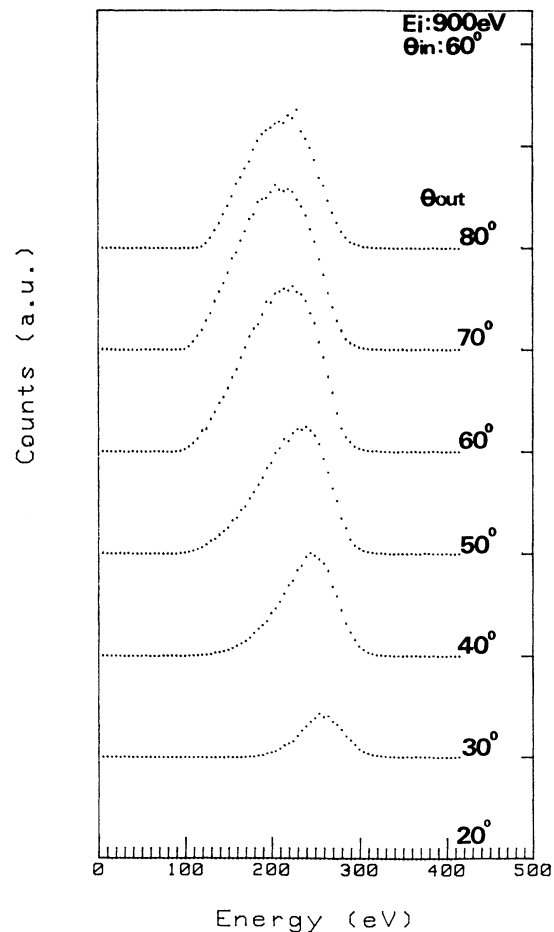


FIG. 4. Exit angle dependence of the scattered  $H^+$  fragment energy spectra for  $H_3^+$  ions with an energy and angle of 900 eV and  $60^\circ$ , respectively.

spectrum of the 1200-eV incident by the following procedure. At incident energies below 1000 eV, the clearly observed surface peak can be sufficiently approximated by a Gaussian line shape, so we assume a similar shape in the high incident energy case. Moreover, as described above, at small exit angles for 1200 eV, the position of the surface-scattered peak agrees with the  $\frac{1}{3}$  energy of the binary scattered  $H_3^+$  from the surface Si atom. Therefore, the surface peak should also be at  $\frac{1}{3}$  the energy of the binary scattered  $H_3^+$  even in spectra at large exit angles. With these assumptions, we extracted the surface peak for 1200-eV incident by fitting the spectrum above  $\frac{1}{3}$  the energy of the binary scattered  $H_3^+$  with a Gaussian line shape. The surface-scattered peak intensity is represented by the area below the fitted Gaussian line and the remainder is the bulk-scattered intensity; the results are shown using a polar representation in Fig. 6. In this figure, the results for 900, 600, and 450 eV are also shown. For the 1200-eV incident, the surface-scattered  $H^+$  beam is intense at exit angles close to the surface parallel. This is reasonable because the differential scattering cross section for binary collisions increases with decreasing scattering angle. But at small exit angles,

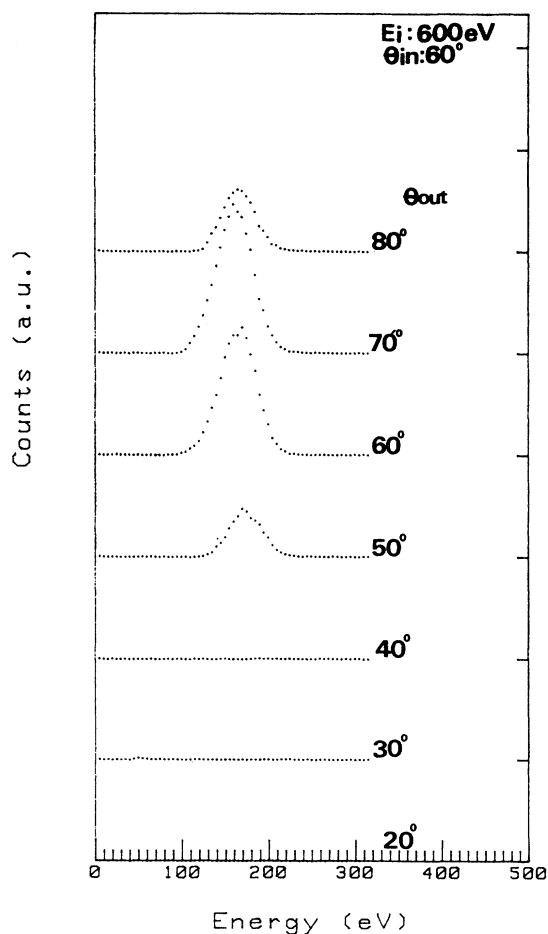


FIG. 5. Exit angle dependence of the scattered  $H^+$  fragment energy spectra for  $H_3^+$  ions with an incident energy and angle of 600 eV and  $60^\circ$ , respectively.

the neutralization probability increases significantly, as predicted by the Hagstrum formula,<sup>17</sup> due to the reduction of the velocity along the surface normal direction. Hence, in the binary collision model, the scattered ion is expected to have an intensity maximum at angles close to the surface parallel. However, specular reflectionlike behavior is clearly observed for incident energy below 1000 eV. The specular lobe becomes sharper with decreasing the incident energy. This specular reflectionlike scattering is caused by the longer interaction range between the incident particles and the surface than the distance between neighboring surface atoms.<sup>7</sup> Therefore, the specular lobe of the scattered  $H^+$  intensity also indicates that the incident  $H_3^+$  interacts with many surface Si atoms at low incident energy.

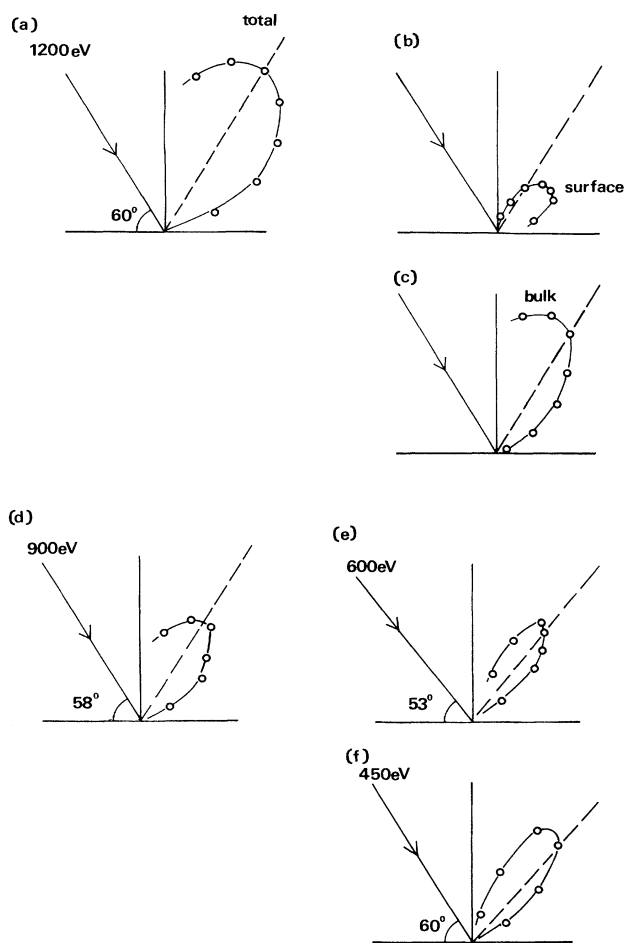


FIG. 6. The surface-scattered  $H^+$  intensity as a function of the exit angles for (b) 1200 eV, (d) 900 eV, (e) 600 eV, and (f) 450 eV  $H_3^+$  incidence. In the 1200-eV  $H_3^+$  case, the exit angle dependence of the totally scattered (including both the surface- and the bulk-scattered) and the bulk-scattered  $H^+$  are also indicated in (a) and (c), respectively. The angular profile is displayed by a polar plot. The arrows mean the incident direction. The broken lines mean the direction of specular reflection.

The disappearance of the bulk scattering, the surface-peak energy shift, and the specular reflectionlike angular distribution of the surface-scattered  $H^+$  intensity mean that the incident  $H_3^+$  interacts with many surface Si atoms in the low incident energy regime. We think that this is due to the long-range interaction potential between the incident  $H_3^+$  and the Si surface. On the other hand, the Thomas-Fermi-Moliere potential<sup>18</sup> is known to well describe the interaction for noble gas ion scattering of the energy in keV range from surfaces. The Thomas-Fermi-Moliere potential represents the strong *short-range* repulsive interaction between the incident ion and the shielded nucleus of the target atom. Here we have assumed that the  $H_3^+$  molecular ion is an ion of  $Z=3$ , and used this potential to calculate the scattering trajectories as a function of the impact parameter. However, the resulting shadow cone for 450-eV incident was too small to explain the disappearance of the bulk scattering. This suggests that the interaction potential between the  $H_3^+$  and the Si surface should have a *long-range* interaction part, as well. Actually, Kasi has reported that the surface scattering of an active atomic ion such as  $O^+$  is well described by the combination of a short-range repulsive Biersack-Ziegler potential and a long-range attractive Morse potential<sup>19</sup> for incident energies below 200 eV. However, for  $H_3^+$  scattering, the long-range potential seems to work even at such a high energy as 1000 eV. One reason for this is the size of the  $H_3^+$  molecular ion; it has a triangular shape and the distance between the proton nuclei is  $0.87 \text{ \AA}$ .<sup>20</sup> Due to this large size,  $H_3^+$  is thought to have a tendency to interact with several target surface Si atoms. We have not yet been able to extract a more precise understanding of the interaction potential.

### B. Dissociation mechanism

As described in Sec. III A,  $H_3^+$  is dissociatively scattered from the Si(100) surface, and the resulting  $H^+$  fragment was detected as a positive scattered ion. For the dissociation, resonant neutralization into the nonbinding ground state of  $H_3$ , energy transfer from translational ( $T$ ) to vibrational ( $V$ ) degrees of freedom, and the dissociation due to the electronic promotion at the close encounter seem to be responsible. In the following, we discuss the possible dissociation mechanism with respect to the magnitude of the kinetic-energy release which causes the characteristic energy broadening of  $H^+$  fragment.

In our experiment, the dissociatively scattered  $H^+$  showed a characteristic Gaussian-like energy broadening. The broad kinetic-energy distribution of the fragment is characteristic of molecular dissociation<sup>10</sup> in which a part of the internal energy of the molecules is released into the kinetic energies of the fragments.<sup>21</sup> Among the several possible dissociation paths for generating  $H^+$  fragments,  $H_3^+ \rightarrow H^+ + H_2$  costs the least energy. Since the second lowest-energy dissociation path  $H_3^+ \rightarrow H^+ + H + H$  costs 5 eV more, here we consider only the dissociation into  $H^+ + H_2$ . At this dissociation, the internal energy  $\Delta E$  is released into the kinetic energy of the fragments. The energy of the  $H^+$  fragment  $E$  is then<sup>21</sup>

$$E = (E_0 + \Delta E \pm \sqrt{\Delta E E_0})/3, \quad (1)$$

where  $E_0$  is the kinetic energy of  $H_3^+$  before the dissociation. In Fig. 7, the calculated energy shift from the central energy ( $E_0/3$ ) is shown as a function of the released energy  $\Delta E$ . As shown in the figure, the effect of the kinetic-energy release is expanded by the third term of Eq. (1). From these results, we think that the observed energy broadening up to  $\sim 100$  eV reflects the distribution of the released energy between 0 and approximately  $\sim 10$  eV. The Gaussian shape of the observed spectrum means the released energy fluctuates about the central value of zero. In Fig. 8, the full width at the half maximum (FWHM) of the surface peak is plotted as a function of the incident energy; the FWHM is deduced from the above-described Gaussian fitting procedure.

First, we discuss the resonant neutralization into the nonbinding ground state. In this experiment, the analyzer detects only positive ions, and precise information on the neutralization was not obtained. But, the scattered  $H^+$  yield was two orders of magnitude smaller than the incident  $H_3^+$  yield. Hence, we believe that most of the scattered particles are neutralized. Such a large neutralization rate has been also reported for  $H_3^+$  scattering from metal surfaces in the energy range below 1 keV.<sup>22,23</sup> In these previous studies, not only  $H^+$  but also  $H_2^+$  and  $H_3^+$  have been observed, whereas only  $H^+$  was observed in our experiment.  $H_2^+$  and  $H_3^+$  have been found to become dominant with decreasing the exit angle (below  $5^\circ$  from the surface) and lowering energy (230 eV).<sup>23</sup> Therefore, the lack of  $H_2^+$  and  $H_3^+$  in our experiment is due to the large exit angles (above  $30^\circ$ ) and the higher incident energy (above 450 eV). But, anyway, even at the previous grazing angle scattering studies, neutrals are more abundant by two orders of magnitude.<sup>22,23</sup> Resonant charge transfer from the surface to the nonbinding  $2p^2E'$  ground state of  $H_3$  seems to be the origin of the large neutralization rate. Electron affinity of  $H_3^+$

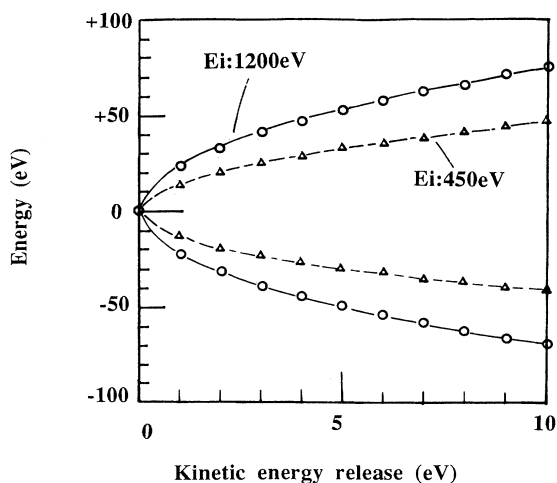


FIG. 7. Calculated energy shift resulting from kinetic-energy release. Results for 1200 and 450 eV are shown. Lines are a guide for the eyes.

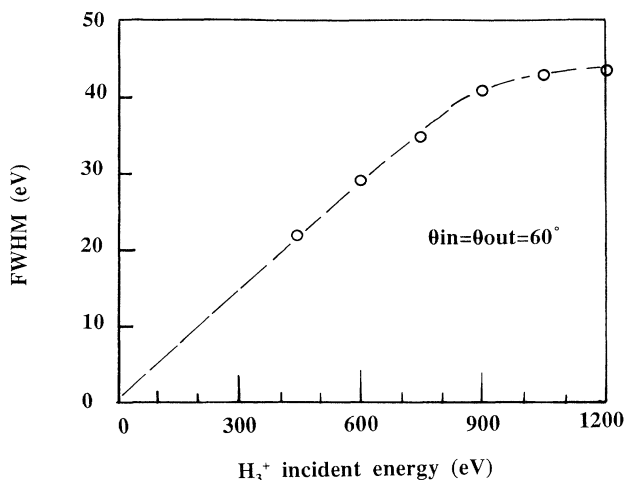


FIG. 8. Incident energy dependence of the observed FWHM of the surface peak. The line is a guide for the eyes.

to the  $2p^2E'$  H<sub>3</sub> ground state is 5.4 eV,<sup>24</sup> and is slightly below the Fermi level of Si. On the other hand, metastable excited states of H<sub>3</sub> ( $2p^2A''_2, 2s^2A'_1$ ) exist slightly above the Fermi level.<sup>23,24</sup> Hence, only the resonantlike charge transfer from Si to the  $2p^2E'$  ground state of H<sub>3</sub> is probable. The  $2p^2E'$  state is nonbinding, and dissociates into H+H<sub>2</sub>. If the resulting H is reionized on its outgoing path, this neutralization causes the H<sup>+</sup> fragment.<sup>23</sup> However, the dissociation of  $2p^2E'$  H<sub>3</sub> into H+H<sub>2</sub> releases energy of ~3 eV. But, our experimental results indicate the released energy distribution centered at 0 eV. As Willerding, Snowdon, and Heiland pointed out, the resulting H<sub>2</sub> fragment should be vibrationally excited to about  $\nu=5$  to account for the energy broadening centered at 0 eV.<sup>23</sup> The vibrationally excited H<sub>2</sub> suggests the importance of an impulse feature of the dissociation such as the  $T$ - $V$  energy transfer. Therefore, we think that the large neutralization rate is caused by the resonant neutralization into the  $2p^2E'$  state, but for the dissociation, impulsive collision is more important than the nonbonding character of the  $2p^2E'$  state.

Next, the classical energy transfer between the translational ( $T$ ) and vibrational ( $V$ ) degrees of freedom<sup>9</sup> and energy transfer with the electronic transition<sup>12</sup> are considered. In the classical picture of  $T$ - $V$  energy transfer, the incident H<sub>3</sub><sup>+</sup> is vibrationally excited by impulsive collision with the surface. If the vibrational excitation exceeds the dissociation limit of the H<sub>3</sub><sup>+</sup> molecular ion, it breaks into H<sup>+</sup> and H<sub>2</sub>. A part of the excited vibrational energy of H<sub>3</sub><sup>+</sup> is transferred into the vibrational freedom of the H<sub>2</sub> fragment, but the rest is released into kinetic energy and broadens the kinetic energy of H<sup>+</sup>. If we treat the  $T$ - $V$  energy transfer classically in the Spectator approximation,<sup>25</sup> the energy transfer from  $T$  to  $V$  is expected to be proportional to the incident energy of H<sub>3</sub><sup>+</sup>.<sup>26</sup> This predicts that the kinetic-energy release is fundamentally proportional to the incident energy. In this case, the linear dependence of the energy broadening is expected from Eq. (1). In fact, as shown in Fig. 8, the

observed broadening shows a linear dependence on the incident energy at energies below 900 eV, though it becomes insensitive at higher incident energies. This means that the impulsive energy-transfer mechanism is responsible for the dissociation at least for low incident energy.

Recently, van Slooten, Andersson, and Kleyn proposed an advanced Spectator model for the surface scattering, which considers the energy transfer between translational ( $T$ ) and rotational ( $R$ ) degrees of freedom.<sup>27</sup> In their model, the dissociation fraction is scaled to  $E\theta^2$ , where  $E$  is the incident energy and  $\theta$  is the scattering angle, respectively. They have shown that the dissociated fraction decreases rapidly around  $mE\theta^2=D_0$  for the ( $T$ - $R$  energy-transfer-mediated) dissociative scattering of H<sub>2</sub><sup>+</sup> from Ag(111). Here,  $m$  is the reduced mass of the system and  $D_0$  is the dissociation energy. Though this  $E\theta^2$  plot is a good test to check the importance of the impulsive energy transfer for the dissociation, the present study does not supply the data for the region of decreasing dissociated fraction due to the lack of scattering data for grazing exit angles by a geometrical restriction. However, in the grazing angle scattering of H<sub>3</sub><sup>+</sup> from Ni(111), a relative yield of H<sup>+</sup> to H<sub>3</sub><sup>+</sup> has been reported to decrease at lower incident energy and much smaller exit angles.<sup>23</sup> This suggests the general scaling of the dissociated fraction of H<sub>3</sub><sup>+</sup> to  $E\theta^2$ , and the importance of the impulsive energy transfer for the dissociation.

However, a simple picture of the energy transfer meets difficulty at large kinetic-energy release. The dissociation energy limit of H<sup>+</sup>+H<sub>2</sub> fragmentation is 4.89 eV above the ground state of H<sub>3</sub><sup>+</sup> ( $1A'_1$ ).<sup>28</sup> Therefore, the H<sub>3</sub><sup>+</sup> is necessary to be vibrationally excited at least ~5 eV to generate a H<sup>+</sup> fragment. But the lowest Rydberg state of H<sub>3</sub><sup>+</sup> ( $3\Sigma_u^+$ ) exists ~6 eV above the ground state H<sub>3</sub><sup>+</sup> ( $1A'_1$ ). Hence, for energy release over 1 eV, an excitation including this Rydberg state is more probable as the origin of the kinetic-energy release. Judging from Fig. 7, the energy broadening over ~30 eV is related to this electronic excitation. On the other hand, in Fig. 8, the FWHM of the energy broadening above ~40 eV becomes insensitive to the incident energy. As described above, the linear dependence of the energy broadening is characteristic of the dissociation mediated by the vibrational excitation. Tentatively, we believe that the insensitive part of the broadening at high incident energy is caused by the opening of the electronic excitation channel. In the surface scattering of molecular ions, electron promotion according to the Fano-Lichten mechanism<sup>29</sup> is generally expected at the close encounter of fast incident ion, where a significant orbital overlap between the target atom and the molecular ion occurs.<sup>10</sup> This enables a Frank-Condon-type electronic excitation of H<sub>3</sub><sup>+</sup> from its ground state ( $1A'_1$ ) to a Rydberg state such as  $3\Sigma_u^+$ . The  $3\Sigma_u^+$  state exists ~1 eV above the dissociation limit of H<sup>+</sup>+H<sub>2</sub>, and is a dissociative excited state. In infrared photodissociation of H<sub>3</sub><sup>+</sup> into H<sup>+</sup>+H<sub>2</sub>, energy release up to 2–3 eV has been reported by the transition from a rotationally and vibrationally excited  $3\Sigma_u^+$ H<sub>3</sub><sup>+</sup> state to several rotationally and vibrationally excited H<sub>2</sub>+H<sup>+</sup> states.<sup>30</sup> Even in this case including electronic excitation,

a continuous kinetic-energy release has been realized by the rich of rotationally and vibrationally excited states of both the excited  $H_3^+$  and the  $H_2$  fragment. Namely, the dissociation has an impulsive feature. In our  $H_3^+$  dissociation by collision with the Si surface, a kinetic-energy distribution up to  $\sim 10$  eV was observed for incident energies above 900 eV. We think that this wide and continuous distribution is due to the dissociation of an electronically and rotationally and vibrationally excited  $H_3^+$  state, which is generated at the closest encounter, into a rotationally and vibrationally excited  $H_2$  and  $H^+$  fragment.

#### IV. CONCLUSION

Dissociative scattering of  $H_3^+$  from the Si(100) surface was studied with incident energies from 450 to 1500 eV. At these energies,  $H_3^+$  was dissociatively scattered and scattered  $H^+$  fragments were observed. For incident energies above 1000 eV, a surface-scattered peak and bulk-scattered feature were observed in the energy spectrum of the  $H^+$  fragments. By reducing the incident energy, the bulk-related scattering became weaker and for incident energies below 1000 eV only the surface-scattered peak was observed. Also, by decreasing the incident energy, the exit angle distribution of the surface-scattered  $H^+$  in-

tensity changed from a binary collisionlike distribution to a specular reflectionlike one. At the same time, the energy of the surface-scattered peak shifted toward a higher energy than that expected from the binary collision model. These changes mean that by decreasing the incident energy the incident  $H_3^+$  starts to feel the long-range potential of many surface Si atoms. At low incident energies below 1000 eV, the surface-scattered  $H^+$  energy spectrum had a Gaussian-like line shape. The width of the surface-scattered peak comes from a kinetic-energy release of up to  $\sim 10$  eV upon dissociative scattering. Resonant neutralization into the nonbinding ground state of  $H_3$ , classical energy transfer from translational to vibrational degrees of freedom upon the scattering, and the dissociation including the electronic excitation into the dissociative Rydberg state are possible origins of the dissociation. The large neutralization rate comes from the dominant neutralization process. But, to realize the observed Gaussian-like broadening, the resulting  $H_2$  fragment should be vibrationally excited. This means that impulsive nature is important for the dissociation.

#### ACKNOWLEDGMENT

The author would like to thank D. Tweet for his critical reading of the manuscript.

- 
- <sup>1</sup>S. R. Kasi, H. Kang, C. S. Sass, and J. W. Rabalais, *Surf. Sci. Rep.* **10**, 1 (1989).
- <sup>2</sup>H. Hirayama, M. Hiroi, K. Koyama, T. Tatsumi, and F. Sato, in *Silicon Molecular Beam Epitaxy*, edited by J. C. Bean, S. S. Iyer, and K. L. Wang, MRS Symposia Proceedings No. 220 (Materials Research Society, Pittsburgh, 1991), p. 545.
- <sup>3</sup>H. Hirayama and T. Tatsumi, *Appl. Phys. Lett.* **54**, 1561 (1989).
- <sup>4</sup>S. M. Gates, C. M. Greenlief, D. B. Beach, and P. A. Holbert, *J. Chem. Phys.* **92**, 3144 (1990).
- <sup>5</sup>H. Hirayama, *Surf. Sci.* **287/288**, 12 (1993).
- <sup>6</sup>D. P. Smith, *J. Appl. Phys.* **38**, 340 (1967).
- <sup>7</sup>J. A. Barker and D. J. Auerbach, *Surf. Sci. Rep.* **4**, 1 (1984).
- <sup>8</sup>H. Akazawa and Y. Murata, *Surf. Sci.* **207**, L971 (1989).
- <sup>9</sup>H. Akazawa and Y. Murata, *J. Chem. Phys.* **92**, 5560 (1990).
- <sup>10</sup>C. S. Sass and J. W. Rabalais, *J. Chem. Phys.* **89**, 3870 (1988).
- <sup>11</sup>B. Willerding, W. Heiland, and K. J. Snowdon, *Phys. Rev. Lett.* **53**, 2031 (1984).
- <sup>12</sup>U. Imke, K. Snowdon, and W. Heiland, *Phys. Rev. B* **34**, 48 (1986).
- <sup>13</sup>W. Heiland, U. Beitata, and E. Taglauer, *Phys. Rev. B* **19**, 1677 (1979).
- <sup>14</sup>R. Souda, T. Aizawa, C. Oshima, S. Otani, and Y. Ishizawa, *Phys. Rev. B* **40**, 4119 (1989).
- <sup>15</sup>R. Souda, W. Hayami, T. Aizawa, S. Otani, and Y. Ishizawa, *Phys. Rev. Lett.* **69**, 192 (1992).
- <sup>16</sup>D. P. Smith, *Surf. Sci.* **25**, 171 (1971).
- <sup>17</sup>H. D. Hagstrum, in *Inelastic Ion-Surface Collisions*, edited by N. H. Tolk, J. C. Tully, W. Heiland, and C. W. White (Academic, New York, 1977).
- <sup>18</sup>A. J. Algra, P. P. Maaskant, S. B. Luitjens, E. P. Th. M. Suurmeyer, and A. L. Boers, *J. Phys. D* **13**, 2363 (1980).
- <sup>19</sup>S. R. Kasi, M. Kilburn, H. Kang, J. W. Rabalais, L. Taverini, and P. Hochmann, *J. Chem. Phys.* **88**, 59 (1988).
- <sup>20</sup>C. E. Dykstra, A. S. Gaylord, W. D. Gwinn, W. C. Swope, and H. F. Schaefer III, *J. Chem. Phys.* **68**, 3951 (1978).
- <sup>21</sup>J. R. Peterson and Y. K. Bae, *Phys. Rev. A* **30**, 2807 (1984).
- <sup>22</sup>J. Laszlo and W. Eckstein, *J. Nucl. Mater.* **184**, 22 (1991).
- <sup>23</sup>B. Willerding, K. Snowdon, and W. Heiland, *Z. Phys. B* **59**, 435 (1985).
- <sup>24</sup>H. F. King and K. Morokuma, *J. Chem. Phys.* **71**, 3212 (1979).
- <sup>25</sup>M. J. Gaillard, D. S. Gemmell, G. Goldring, I. Levine, W. J. Pietsch, J. C. Poizat, A. J. Ratkowski, J. Remillieux, Z. Vager, and B. J. Zabransky, *Phys. Rev. A* **17**, 1797 (1978).
- <sup>26</sup>B. H. Mahan, *J. Chem. Phys.* **52**, 5221 (1970).
- <sup>27</sup>U. van Slooten, D. R. Andersson, and A. W. Kleyn, *Surf. Sci.* **274**, 1 (1992).
- <sup>28</sup>H. van Dop, A. J. H. Boerboom, and J. Los, *Physica* **54**, 223 (1971).
- <sup>29</sup>U. Fano and W. Lichten, *Phys. Rev. Lett.* **14**, 627 (1965).
- <sup>30</sup>A. Carrington and R. A. Kennedy, *J. Chem. Phys.* **81**, 91 (1984).